3D CURVE INTERPOLATION AND OBJECT RECONSTRUCTION

S. H. Baloch*, H. Krim*, W. Mio†, A. Srivastava‡

*ECE Dept., NCSU, Raleigh, NC.
†Dept. of Math., FSU, Tallahassee, FL.
‡Dept. of Stat., FSU, Tallahassee, FL.

ABSTRACT

Three dimensional objects viewed as surfaces or volumes embedded in $\mathbb{R}^3$, are usually sampled along the z-dimension by planes for rendering or modeling purposes. The resulting intersections are curves or planar shapes which may in turn be modeled for parsimony of representation. Each curve or planar shape may be viewed as a point in a high dimensional manifold, thereby providing the notion of interpolation between two curves or two points on this manifold to reconstruct the subsurface that lies between the two slices. We exploit some recent results in formulating this interpolation problem as an optimization problem in $\mathbb{R}^3$ to yield a simple interpolating spline, known as elasticæ, which when evaluated at intermediate points yields curves which can in turn be instrumental in 3D reconstruction. The approach is particularly suited for interpolation between MRI slices and for modeling and reconstruction of 3D shapes.

1. INTRODUCTION

Interpolation has long been of interest in Signal Processing, since it is the very basis of signal reconstruction from discrete sampled data. Linear and nonlinear interpolation have witnessed a development of a wealth of techniques using wavelets and splines[1, 3] just to name a few. In all these studies, the interpolation was point-wise and the local inter-sample correlation was to a large extent overlooked. A natural generalization of this approach may for instance, define an algebraically coupled set of samples (e.g. forming a curve) as a starting point, to be interpolated to another similarly defined set of samples (i.e. a curve to another). Such curves are typically the result of sampling a surface embedded in $\mathbb{R}^3$ along the z-dimension with a flat plane, as shown in Fig. 1. They are, hence, intersections of parallel planes with a surface. Applications where such cross-sectional data arise, include medical imaging, microscopy, manufacturing, geology and more.

In particular, digital 3D reconstruction techniques based on interpolating 2D slices are not only encountered in Magnetic Resonance Imaging applications but also in terrain modeling from topographic elevation contour information [2]. A myriad of methods addressing different aspects of these problems have been proposed in the literature[11, 2]. In trying to contiguously connect various curves and to allow for possible topological changes, one is indeed faced with physical branching and bifurcation of a surface referred to as the *correspondence* and *branching* problems.

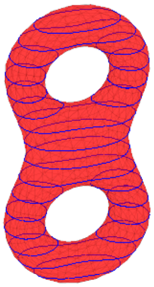

Fig. 1. *Vertical sampling of a surface.*

In [6], Jones and Chen proposed a reconstruction technique that solves these problems in a simple and elegant way. They subsequently proceed to linearly interpolate the distance of various slices to obtain a function F defined on a 3D space. The desired 3D model is then obtained as the 0-level set of F.

Many good 3D models in surface/object reconstruction have been proposed in the literature [4, 11] and their overlooking of other than adjacent slices which ignores information about the overall shape causes severe artifacts (sharp edges and artifacts). In this paper, we seek to refine existing methods and using [6] as an inspiration, we exploit recent results in Mio *et. al.*[8] and propose the notion of *elasticæ* to naturally describe the evolution of two curves. In addition, this proposed technique seeks to only preserve singularities present in the input data. This is achieved with no significant change in the typically sparse nature of the data.

The novelty of this approach lies in our introduction of an energy functional on the distance fields of the level curves which is intuitively appealing and sensible and generalizes the linear interpolation of [6]. Specifically, we maintain that a smooth displacement of these distance fields (which amount to a smooth evolution of cross-section curves) is *almost always* the prevailing law of nature, and hence justifies the choice of an *elasticæ* function for interpolating them in a function space. This infinite dimensional space is challenging to optimize over, and hence, requires a judicious formulation by constraining the problem to a 3D subspace where the interpolation curve, i.e.,

This work was supported by AFOSR F49620-98-1-0190 and NSF CCR-9984067 grants.

the elasticæ solution, will lie [7, 8].

2. INTERPOLATION MODELS

2.1. The Linear Model

Recall that sample curves/cross-sectional data are typically a result of intersections of a surface with a plane along a $z-$ dimension in a Euclidean coordinate system. Since all practical surfaces of interest are compact, it is natural to assume that all intersections lie within a fixed bounded region Ω of the plane $\mathbb{R}^2$, i.e. a sufficiently large enclosing rectangle. More precisely, a cross-section $\mathcal{R}$ at level z is assumed to be contained in $\Omega \times \{z\}$. When the z-level is not relevant, we may think of cross-sections simply as subsets of Ω.

Generically, the contour $\mathcal{C}$ of a cross-section $\mathcal{R} \subseteq \Omega$ consists of a collection of non-overlapping closed curves.[1] Associated with $\mathcal{R}$, there is a signed distance field $\rho\colon \Omega \to \mathbb{R}$ as illustrated in Fig. 2, given by:

$$\rho(x,y) = \left\{ \begin{array}{ll} +D((x,y),\mathcal{C}), & \text{if } (x,y) \notin \mathcal{R}; \\ -D((x,y),\mathcal{C}), & \text{if } (x,y) \in \mathcal{R}, \end{array} \right. \tag{1}$$

where $D((x,y),\mathcal{C})$ denotes the distance from any point $(x,y) \in \Omega$ to the set $\mathcal{C}$, i.e.,

$$D((x,y),\mathcal{C}) = \min_{u,v \in \mathcal{C}} d\left((x,y),(u,v)\right).$$

The contour $\mathcal{C}$ may be viewed as the isoset $\mathcal{C} = \rho^{-1}(0)$. Just as $\mathcal{C}$ is sometimes viewed as a subset of $\Omega \times \{z\}$, we often think of ρ as defined on $\Omega \times \{z\}$.

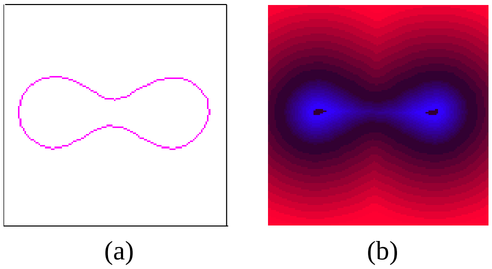
(a) (b)

Fig. 2. *Distance field representation of a curve: (a) Original curve; (b) Distance field. Red corresponds to exterior while blue corresponds to the interior of the curve where the field is negative.*

As pictorially illustrated in Fig. 1, we are given K cross-sections $\mathcal{R}_i$ of an object (e.g. a double torus) $0 \le i \le K-1$, from horizontal slices at levels z_i, with $z_{i-1} < z_i$, and we let ρ_i denote the associated distance fields. The problem is to reconstruct a surface given the slices.

Jones and Chen [6] linearly interpolate consecutive distance fields $\rho_i\colon \Omega \times \{z_i\} \to \mathbb{R}$ to obtain a function $F\colon \Omega \times [z_0, z_{K-1}] \to \mathbb{R}$. The contour $\mathcal{S}$ of the 3D object is reconstructed as the isosurface $\mathcal{S} = F^{-1}(0)$, and practically extracted using the *Marching Cubes Algorithm* [12].

2.2. Problem Formulation

In practice, Ω is finite dimensional and ordering its n pixels yields a function $\boldsymbol{\rho} : \Omega \to \mathbb{R}^n$ which in turn may be represented by an n-tuple $(d_1, \ldots, d_n) \in \mathbb{R}^n$.

Let the distance field corresponding to the intersection curve at level z_i be $\boldsymbol{\rho}_i \equiv (d_1^i, \ldots, d_n^i)$. For K intersections, we get an ordered collection $\{\boldsymbol{\rho}_i, 0 \le i \le K-1\}$ of points in $\mathbb{R}^n$, and would like to model a trajectory that passes through them. The trajectory will then be used to interpolate between the given points to reconstruct the entire surface from the given intersections. The linear interpolation used by Jones and Chen corresponds to a polygonal curve in $\mathbb{R}^n$ connecting these points as illustrated in Fig. 3(a). A linear evolution of curves is clearly overoptimistic in the sense that it completely ignores any dependence of the end curves on their immediate neighbors and that the distance fields typically lie in some curved space. In contrast, we seek to replace this linear interpolation by an elasticæ fulfilling nonlinear curve to join these fields on this manifold. The elasticæ is formulated in a way that it introduces the notion of dependence of any curves interpolated close to the end points on their immediate neighbors. This is achieved by imposing the starting and ending point tangent constraints as illustrated in Fig 3(b). As shown in Fig.3, elasticæ also ensures smoothness at the junctions.

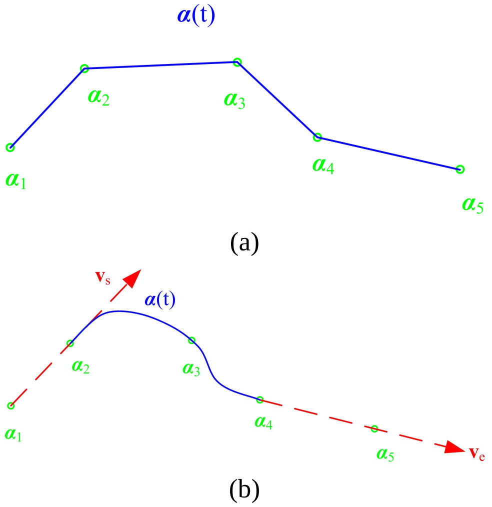

(a)

(b)

Fig. 3. *Approximation of an interpolation curve in* $\mathbb{R}^3$*: (a) Linear approximation; (b) Nonlinear fit.*

2.3. Nonlinear Interpolation

The interpolations we wish to consider consist of $K-1$ smooth arcs in $\mathbb{R}^n$ connecting $\boldsymbol{\rho}_{i-1}$ to $\boldsymbol{\rho}_i$, $1 \le i \le K$, whose tangent vectors agree at the junctions. By requiring that the tangent vectors to the curve at the i^{th} and $(i+1)^{th}$ junctions assume some direction and that the displacement between the two distance fields be upper-bounded, we are in effect stating that the solution curve lie in a 3D subspace with canonical directions given by these three vectors. The direction of the tangent vec-

[1] Note that we do not restrict the topology of the surface being reconstructed, which could in fact have holes and branches.

tor at the i^{th} and $(i+1)^{th}$ junction is given by:

$$\mathbf{v}_i = \frac{\boldsymbol{\rho}_{i+1} - \boldsymbol{\rho}_{i-1}}{\|\boldsymbol{\rho}_{i+1} - \boldsymbol{\rho}_{i-1}\|},$$

for $0 < i < K-1$. For generic objects, we can suppose that the displacement vectors $\boldsymbol{\rho}_{i+1} - \boldsymbol{\rho}_{i-1} \neq 0$, for every $0 < i < K-1$, so that $\mathbf{v}_i$ is well defined, computed as shown in Fig. 4.

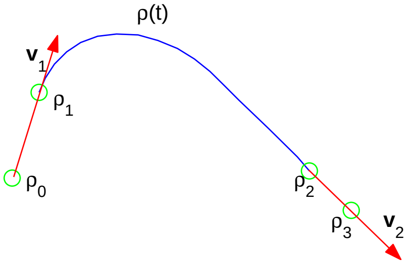

Fig. 4. *Approximation of tangents for a solution in* $\mathbb{R}^3$.

At the initial and terminal points, as illustrated in Fig. 3(b), we use:

$$\mathbf{v}_0 = \frac{\boldsymbol{\rho}_1 - \boldsymbol{\rho}_0}{\|\boldsymbol{\rho}_1 - \boldsymbol{\rho}_0\|} \quad \text{and} \quad \mathbf{v}_K = \frac{\boldsymbol{\rho}_K - \boldsymbol{\rho}_{K-1}}{\|\boldsymbol{\rho}_K - \boldsymbol{\rho}_{K-1}\|}, \tag{2}$$

which we also assume to be well defined. For space reasons, other special cases are omitted and discussed elsewhere.

With this formulation in hand, we may succinctly state the interpolation problem as follows: for each $1 \leq i \leq K-1$, find the most "energy efficient" unit-speed curve $\boldsymbol{\alpha}_i$ in $\mathbb{R}^n$ having $\boldsymbol{\rho}_{i-1}$ and $\boldsymbol{\rho}_i$ as initial and terminal points, and $\mathbf{v}_{i-1}$ and $\mathbf{v}_i$ as initial and terminal velocity vectors, respectively. The issue of energy efficiency brings us to the notion of *elasticæ*.

2.4. The elasticæ model

Let $\boldsymbol{\alpha}\colon [0,L] \longrightarrow \mathbb{R}^n$ be a unit-speed curve in $\mathbb{R}^n$. The curvature of $\boldsymbol{\alpha}$ at $s \in [0,L]$ is given by $\kappa(s) = \|\boldsymbol{\alpha}''(s)\|$. The (bending) *elastic energy* of $\boldsymbol{\alpha}$ is defined by:

$$E(\boldsymbol{\alpha}) = \int_0^L \kappa^2(s)\, ds.$$

These functionals date back to Euler [5] and were introduced in computer vision by Mumford to model edge occlusions [9]. It is often the case that, in pattern recognition problems, it is more natural to use a *scale invariant* form of the elastic energy. Such functional was introduced in [11, 4] and is given by:

$$E_{si}(\alpha) = L\int_0^L \kappa^2(s)\, ds.$$

We may now state the interpolation problem as:
Given points $\mathbf{p}, \mathbf{q} \in \mathbb{R}^n$ *and unit vectors* $\mathbf{v}_1, \mathbf{v}_2 \in \mathbb{R}^n$, *find a unit-speed curve* $\boldsymbol{\alpha}$ *in* $\mathbb{R}^n$ *of minimal scale-invariant elastic energy having* $\mathbf{p}, \mathbf{q}$ *as initial and terminal points, and* $\mathbf{v}_1, \mathbf{v}_2$ *as initial and terminal velocity vectors.*

The energy minimizing curves satisfying first-order boundary conditions are called *scale-invariant elasticæ*. Minimizing the bending energy results in a curve which is smooth. In the absence of any tangent constraints, the solution will be a straight line joining the two points and we are left with the interpolation of Jones *et. al*. Fixing the tangents constrains the launching and ending directions of the velocity vector along the curve and the minimization of the bending energy results in a curve that is least bent. In other words, elasticæ generalizes the linear interpolation, and when the two tangents are perfectly aligned, we converge to the same solution.

In the planar case, algorithms to compute curves that approximate elasticæ were studied in [10]. Fast algorithms to compute scale-invariant and other forms of elasticæ in $\mathbb{R}^n$ were developed in [8]. An illustration of fitting a trajectory through successive level curves is given in Fig. 5.

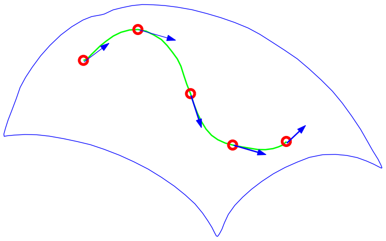

Fig. 5. *A trajectory on an* $(n-1)$*-manifold to model curves represented as points in* $\mathbb{R}^n$.

2.5. Elasticæ in $\mathbb{R}^3$

Instead of minimizing the bending energy in high dimensional space, the given constraints may be fulfilled by projecting the tangents $\mathbf{v}_1, \mathbf{v}_2$ and the displacement $\mathbf{d} = \mathbf{q} - \mathbf{p}$ to $\mathbb{R}^3$, thus reducing significantly the computational cost. Assume that $\{\mathbf{v}_1, \mathbf{v}_2, \mathbf{d}\}$ forms a linearly independent set. A Gram-Schmidt orthogonalization results in:

$$\begin{aligned} \mathbf{b}_1 &= \mathbf{v}_1; \\ \mathbf{b}_2 &= \frac{\mathbf{v}_2 - \langle \mathbf{v}_2, \mathbf{b}_1\rangle \mathbf{b}_1}{\|\mathbf{v}_2 - \langle \mathbf{v}_2, \mathbf{b}_1\rangle \mathbf{b}_1\|}; \\ \mathbf{b}_3 &= \frac{\mathbf{d} - \langle \mathbf{d}, \mathbf{b}_1\rangle \mathbf{b}_1 - \langle \mathbf{d}, \mathbf{b}_2\rangle \mathbf{b}_2}{\|\mathbf{d} - \langle \mathbf{d}, \mathbf{b}_1\rangle \mathbf{b}_1 - \langle \mathbf{d}, \mathbf{b}_2\rangle \mathbf{b}_2\|}. \end{aligned} \tag{3}$$

$\{\mathbf{b}_1, \mathbf{b}_2, \mathbf{b}_3\} \subset \mathbb{R}^n$ forms an orthonormal set. Let $\mathbf{e}_1, \mathbf{e}_2, \mathbf{e}_3$ be the canonical basis for $\mathbb{R}^3$. We project $\mathbf{v}_1, \mathbf{v}_2$ and $\mathbf{d}$ to $\mathbb{R}^3$ according to the following:

$$\begin{aligned} \mathbf{w}_1 &= \mathbf{e}_1; \\ \mathbf{w}_2 &= \langle \mathbf{v}_2, \mathbf{b}_1\rangle \mathbf{e}_1 + \langle \mathbf{v}_2, \mathbf{b}_2\rangle \mathbf{e}_2 + \langle \mathbf{v}_2, \mathbf{b}_3\rangle \mathbf{e}_3; \\ \mathbf{w}_3 &= \langle \mathbf{d}, \mathbf{b}_1\rangle \mathbf{e}_1 + \langle \mathbf{d}, \mathbf{b}_2\rangle \mathbf{e}_2 + \langle \mathbf{d}, \mathbf{b}_3\rangle \mathbf{e}_3. \end{aligned} \tag{4}$$

The problem is now simplified to finding elasticæ $\boldsymbol{\alpha} : I = [0,1] \longrightarrow \mathbb{R}^3$ satisfying $\boldsymbol{\alpha}(0) = \mathbf{0}$, $\boldsymbol{\alpha}(1) = \mathbf{w_3}$ with starting and ending tangents $\frac{\boldsymbol{\alpha}'(0)}{\|\boldsymbol{\alpha}'(0)\|} = \mathbf{w}_1$ and $\frac{\boldsymbol{\alpha}'(1)}{\|\boldsymbol{\alpha}'(1)\|} = \mathbf{w}_2$ respectively. Each point $\boldsymbol{\alpha}(t) \in \mathbb{R}^3$ may be viewed as a position vector $\boldsymbol{\rho}(t) \in \mathbb{R}^n$ according to:

$$\boldsymbol{\rho}(t) = \mathbf{p}_1 + \langle \boldsymbol{\alpha}(t), \mathbf{e}_1\rangle \mathbf{b}_1 + \langle \boldsymbol{\alpha}(t), \mathbf{e}_2\rangle \mathbf{b}_2 + \langle \boldsymbol{\alpha}(t), \mathbf{e}_3\rangle \mathbf{b}_3. \tag{5}$$

Clearly, $\boldsymbol{\rho}(t)$ given by Eq. (5) satisfies the tangent and displacement constraints.

2.6. Algorithm

The algorithm may then be summarized as follows:

- Given $\boldsymbol{\rho}_{k-1}, \boldsymbol{\rho}_k, \mathbf{v}_{k-1}, \mathbf{v}_k$, let $\boldsymbol{\alpha}_k \colon [0, L_k] \to \mathbb{R}^n$ be the scale-invariant elasticæ satisfying the boundary conditions in Eq. 2.
- For each $t \in [0, L_k]$, $\boldsymbol{\alpha}_k(t) \in \mathbb{R}^n$ represents a function $\Omega \to \mathbb{R}$, whose value at the (i, j)-th pixel $p_{ij} \in \Omega$ will be denoted $\alpha_k(t)(p_{ij})$.
- Define $F_k \colon \Omega \times [z_{k-1}, z_k] \to \mathbb{R}$ by:

  $$F_k(p_{ij}, z) = \alpha_k(t)(p_{ij}),$$

  where $t = \frac{L_k}{z_k - z_{k-1}}(z - z_{k-1})$. Stacking the F_k's, we obtain $F \colon \Omega \times [z_0, z_{K-1}] \to \mathbb{R}$, or more precisely, a function F defined on the voxels of $\Omega \times [z_0, z_{K-1}]$.
- As in [6], using the *Marching Cubes Algorithm* [12], we extract the isoset $F^{-1}(0)$, which yields the *elasticæ model* of the 3D object we are to reconstruct.

3. EXAMPLES

In this section, we present some examples where we reconstruct 3D objects given respective sets of slices. Slices for double torus, as shown in Fig. 1, were used to reconstruct a double torus given in Fig. 7(a).

In Figs. 6(a) and (b), a vase and its level curves are shown, which were used to reconstruct a vase illustrated in Fig.7(b). Note that the surface is rendered using the Marching Cube algorithm.

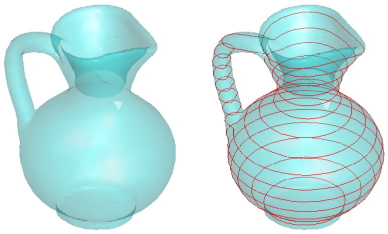

(a) (b)

Fig. 6. *3D object and its level curves: (a) Vase; (b) Level curves.*

4. REFERENCES

[1] A.P. Pentland,*Interpolation Using Wavelet Bases* IEEE Trans. on Pattern Analysis and Machine Intelligence, Vol 16, No. 4, pp. 410-414, 1994.

[2] A.T. Fomenco and T.L. Kunii, *Topological modeling for visualization*, Springer-Verlag Tokyo, 1997.

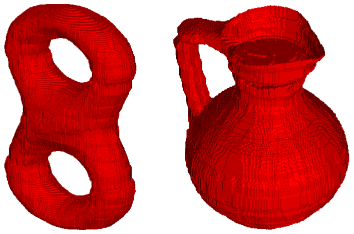

(a) (b)

Fig. 7. *3D object reconstruction using elasticæ: (a) Double torus; (b) Vase.*

[3] Vaidyanathan, P. P., Multirate systems and filter banks, Prentice Hall, New Jersey,1992

[4] A. M. Bruckstein and A. N. Netravali, *On minimal energy trajectories*, Computer Vision, Graphics and Image Processing **49** (1990), 283–296.

[5] L. Euler, *Methodus inveniendi lineas curvas maximi minimive proprietate gaudentes, sive solutio problematis isoperimetrici lattisimo sensu accepti*, Bousquet, Lausannae e Genevae (1744) E65A. O. O. Ser. I, vol. 24.

[6] M. W. Jones and M. Chen, *A new approach to the construction of surfaces from contour data*, Computer Graphics Forum **13** (1994), C75–C84.

[7] J. Langer and D. A. Singer, *The total squared curvature of closed curves*, J. Differential Geometry **20** (1984), 1–22.

[8] W. Mio, A. Srivastava, and E. Klassen, *Interpolations with elasticæ in Euclidean spaces*, to appear in Quarterly of Applied Mathematics.

[9] D. Mumford, *elasticæ and computer vision*, in Algebraic Geometry and its Applications (West Lafayette, IN, 1990), 491–506, Springer, New York, 1994.

[10] E. Sharon, A. Brandt and R. Basri, *Completion energies and scale*, IEEE Trans. Pattern Analysis and Machine Intelligence **15** (2000), 1117–1131.

[11] I. Weiss, *3D shape representation by contours*, Computer Vision, Graphics and Image Processing **41** (1988), 80–100.

[12] , W.E. Lorensen and H. E. Cline, A high resolution 3D surface construction Algorithm, Proceedings of SIGGRAPH'87, Vol 21, No. 4, pp. 163-169.